Journal of Zhejiang University-SCIENCE C (Computers & Electronics)
ISSN 1869-1951 (Print); ISSN 1869-196X (Online)
www.zju.edu.cn/jzus; www.springerlink.com
E-mail: jzus@zju.edu.cn

Coordinated standoff tracking of moving targets using differential geometry*

Zhi-qiang SONG[1,2], Hua-xiong LI[†‡1], Chun-lin CHEN[1], Xian-zhong ZHOU[1], Feng XU[3]

([1]*Department of Control and System Engineering, School of Management and Engineering, Nanjing University, Nanjing 210093, China*)

([2]*Department of Information, Suzhou Institute of Trade and Commerce, Suzhou 215009, China*)

([3]*No. 207 Research Institute, China North Industries Group Corporation, Taiyuan 030006, China*)

[†]E-mail: huaxiongli@nju.edu.cn

Received Oct. 14, 2013; Revision accepted Jan. 7, 2014; Crosschecked Mar. 17, 2014

Abstract: This research is concerned with coordinated standoff tracking, and a guidance law against a moving target is proposed by using differential geometry. We first present the geometry between the unmanned aircraft (UA) and the target to obtain the convergent solution of standoff tracking when the speed ratio of the UA to the target is larger than one. Then, the convergent solution is used to guide the UA onto the standoff tracking geometry. We propose an improved guidance law by adding a derivative term to the relevant algorithm. To keep the phase angle difference of multiple UAs, we add a second derivative term to the relevant control law. Simulations are done to demonstrate the feasibility and performance of the proposed approach. The proposed algorithm can achieve coordinated control of multiple UAs with its simplicity and stability in terms of the standoff distance and phase angle difference.

Key words: Unmanned aircraft, Standoff tracking, Differential geometry, Coordinated control
doi:10.1631/jzus.C1300287 **Document code:** A **CLC number:** TP13

1 Introduction

Unmanned aircrafts (UAs) can be employed in a wide variety of military and civilian applications (Nigam *et al.*, 2012; Ping *et al.*, 2012; Acevedo *et al.*, 2013; Forsmo *et al.*, 2013; Zarea *et al.*, 2013). Military forces face great challenges to provide continuous information on a target of interest. Multiple UAs have the potential to revolutionize military applications due to their ability to coordinate with each other in order to achieve common goals. Missions involving multiple UAs, each equipped with communication, sensing, computation, and control capabilities, can be robustly designed to provide better results than these involving a single UA. For some applications such as exploration, persistent surveillance, search and rescue, border patrol, vehicle convoy, and area coverage, multiple coordinated UAs can provide more accurate target positioning than a single UA. Cooperation between multiple UAs can improve performance in terms of search efficiency, execution time, and system robustness. In these applications, target tracking or surveillance is one of the crucial UA properties required.

It is necessary to acquire exact target position information, as well as to track and monitor a target without being detected. This can be achieved by tracking the target using multiple UAs, keeping a certain distance from the target and a predetermined angular separation between UAs. The distance from the target is called the 'standoff distance' and this type of tracking is known as 'standoff tracking'. The target can be stationary or moving. Lawrence (2003) was the first to propose Lyapunov guidance vector field

‡ Corresponding author

* Project supported by the National Natural Science Foundation of China (Nos. 61273327 and 71201076), the Key Pre-research Fund of the PLA General Armament Department (No. 9140A06050213BQX), and the Natural Science Foundation of Jiangsu Province, China (No. BK2011564)

for standoff tracking. Wise and Rysdyk (2006) well reviewed and compared several different approaches for tracking a moving target with multiple UAs. Further research on Lyapunov vector field was conducted by Frew *et al.* (2008) and Lawrence *et al.* (2008) to consider phase keeping for two UAs as well as standoff distance keeping. Summers *et al.* (2009) further developed the Lyapunov guidance vector field approach to guide multiple UAs to a desired circle and used a variable airspeed control law which achieved the desired phase angle using information architectures. Lim *et al.* (2013) extended Frew *et al.*'s work to achieve simultaneous capture by using a modified vector field and keeping various phases among the UAs by using a standoff distance command and a speed command. The Lyapunov vector field was constructed by representing a desired heading and desired velocity. Chen *et al.* (2013) developed the T+LVFG algorithm which is a hybrid algorithm of tangent vector field guidance (TVFG) and Lyapunov vector field guidance (LVFG). This method allows the UA to reach the standoff circle faster. In addition, Kim *et al.* (2013) proposed a model-based predictive control for coordinated standoff tracking.

Recently, Oh *et al.* (2013) adopted differential geometry based guidance laws for rendezvous and standoff tracking. Our research is aimed to extend Oh *et al.*'s work to improve the performance. We present a control scheme for multiple UAs for the coordinated standoff tracking of a moving target. This scheme uses the associated geometry of the target and the UA. The tangent points of the standoff circle can be easily obtained if the UA is outside the circle. We further develop the differential geometry approach to guide UAs to the desired orbit. The coordinated standoff tracking presented here assumes that the UA is equipped with an on-board Global Positioning System (GPS) and a moving target indicator radar (MTIR). Using our approach, estimates for vehicle location can be acquired by the on-board GPS and MTIR. Using differential geometry, convergent solutions can be obtained depending on the initial positions and the velocity ratio between the UA and the target. Then, a guidance law for coordinated standoff tracking is derived using this convergent solution. Numerical simulations are presented to demonstrate the feasibility of our guidance law. The proposed guidance law based on differential geometry has been shown to have several advantages. First, it is very simple to implement and requires little communication. Second, unlike the state-of-the-art methods, our proposed guidance law can analyze the stability of standoff tracking for a moving target. Third, the proposed algorithm is superior to the algorithm proposed by Oh *et al.* (2013) with a smaller residual error, as demonstrated by simulation results. Although originally motivated by coordinated standoff tracking by multiple UAs, the algorithm presented here is applicable to tracking applications consisting of unmanned surface vehicles, and unmanned ground vehicles under certain circumstances.

2 Relevant differential geometry

The research presented here restricts the analysis to track a constant velocity target in two dimensions. Standoff tracking consists of following and orbiting around a stationary or moving target with a specified standoff distance from the target. We adopt R_0 as the standoff distance (Fig. 1). Standoff tracking geometry is built around the Frenet-Serret frame (White *et al.*, 2007). The desired relative velocity vector of the UA with respect to the target is given by

$$\boldsymbol{V}_{\mathrm{d}} = \hat{\boldsymbol{V}}_1 - \boldsymbol{V}_2, \tag{1}$$

where $\hat{\boldsymbol{V}}_1$ is the desired velocity vector of the UA and $\boldsymbol{V}_2$ is the velocity vector of the target.

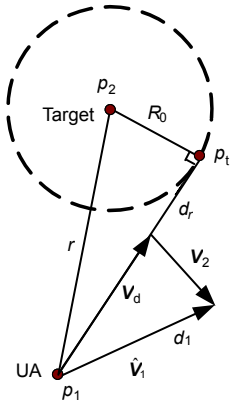

Fig. 1 Relative velocity for standoff tracking

Define $\boldsymbol{t}$ and $\boldsymbol{n}$ as the unit tangent vector and unit normal vector of each UA, respectively. The velocity

vector $\boldsymbol{V}$ over time t, $\boldsymbol{V}=\boldsymbol{V}(t)$, is expressed as a multiple $v=v(t)$ of the unit tangent vector $\boldsymbol{t}$, i.e., $\boldsymbol{V}=v\boldsymbol{t}$. The unit normal vector is orthogonal to $\boldsymbol{t}$ and can be obtained by differentiating $\boldsymbol{t}$. The geometry for standoff tracking shown in Fig. 2 can be expressed as

$$d_1\hat{\boldsymbol{t}}_1 = d_r\boldsymbol{t}_\mathrm{d} + d_2\boldsymbol{t}_2\,, \tag{2}$$

where d_r is a distance from the UA to the tangent point p_t, and d_1, d_2 are the resultant lengths of the unit tangent vectors. Define the speed ratio α of the UA to the target as

$$\alpha = \frac{v_1}{v_2} = \frac{d_1}{d_2} > 1\,, \tag{3}$$

where v_1 and v_2 are the speed of the UA and the target, respectively. Eq. (2) can be rewritten as

$$\hat{\boldsymbol{t}}_1 = \frac{1}{\alpha}\left(\frac{d_r}{d_2}\boldsymbol{t}_\mathrm{d} + \boldsymbol{t}_2\right). \tag{4}$$

In general, for any UA outside a standoff circle with radius R_0, we can easily calculate the two tangent points on the standoff circle. As shown in Fig. 2, p_t at $(x_{p_\mathrm{t}}, y_{p_\mathrm{t}})$ is one of the two tangent points, and we can obtain

$$\begin{cases} x_{p_\mathrm{t}} = \dfrac{R_0^2}{r^2}(x_\mathrm{u}-x_\mathrm{t}) + \dfrac{R_0}{r^2}(y_\mathrm{u}-y_\mathrm{t})\sqrt{r^2-R_0^2} + x_\mathrm{t}, \\ y_{p_\mathrm{t}} = \dfrac{R_0^2}{r^2}(y_\mathrm{u}-y_\mathrm{t}) - \dfrac{R_0}{r^2}(x_\mathrm{u}-x_\mathrm{t})\sqrt{r^2-R_0^2} + y_\mathrm{t}, \end{cases} \tag{5}$$

where the UA is at $(x_\mathrm{u}, y_\mathrm{u})$, and the target is at $(x_\mathrm{t}, y_\mathrm{t})$, $r = \sqrt{(x_\mathrm{u}-x_\mathrm{t})^2 + (y_\mathrm{u}-y_\mathrm{t})^2}$.

In the triangle constructed by $\{p_1, p_\mathrm{t}, p_\mathrm{d}\}$, applying the cosine law leads to

$$d_1^2 = d_r^2 + d_2^2 - 2d_r d_2\cos\theta_\mathrm{d1}\,. \tag{6}$$

With Eq. (3), we can determine

$$\left(\frac{d_r}{d_2}\right)^2 - 2\cos\theta_\mathrm{d1}\left(\frac{d_r}{d_2}\right) - (\alpha^2-1) = 0\,, \tag{7}$$

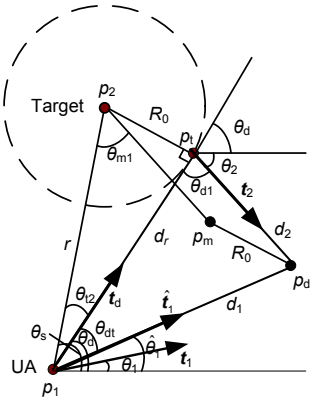

Fig. 2 Geometry for standoff tracking

where

$$d_r = \sqrt{r^2 - R_0^2}\,, \tag{8}$$

$$\theta_\mathrm{d1} = \theta_\mathrm{m1} + \theta_\mathrm{t2}\,. \tag{9}$$

Substituting

$$\cos\theta_\mathrm{t2} = d_r / r = \sqrt{r^2 - R_0^2}\,/\,r\,, \tag{10}$$

$$\sin\theta_\mathrm{t2} = R_0 / r \tag{11}$$

into

$$\begin{aligned}\cos\theta_\mathrm{d1} &= \cos(\theta_\mathrm{m1} + \theta_\mathrm{t2}) \\ &= \cos\theta_\mathrm{m1}\cos\theta_\mathrm{t2} - \sin\theta_\mathrm{m1}\sin\theta_\mathrm{t2}\,,\end{aligned} \tag{12}$$

we have

$$\cos\theta_\mathrm{d1} = \frac{\sqrt{r^2-R_0^2}}{r}\cos\theta_\mathrm{m1} - \frac{R_0}{r}\sin\theta_\mathrm{m1}\,. \tag{13}$$

The shape of the triangle $\{p_1, p_\mathrm{t}, p_\mathrm{d}\}$ is fixed, and will shrink as the UA approaches p_t. Then Eq. (7) will have a fixed solution:

$$d_r / d_2 = \cos\theta_\mathrm{d1} + \sqrt{\alpha^2 - \sin^2\theta_\mathrm{d1}}\,. \tag{14}$$

Another solution is discarded because it is a negative result.

3 Guidance law for standoff tracking

3.1 UA kinematic model

We assume that each UA is equipped with a flight control system (FCS) and the FCS has two layers, a high level guidance layer and a low level control layer. The guidance layer generates the commands and the control layer controls actuators to

execute the guidance commands. We assume that the lower layer controller can track the course and the speed well, as demonstrated by Griffiths (2006) and Nelson *et al.* (2007). Our current research aims to focus on the higher layer and the design of UA guidance inputs to the lower layer controller based on the 2D kinematic model (Kim *et al.*, 2013):

$$\begin{bmatrix}\dot{x}\\ \dot{y}\\ \dot{\psi}\\ \dot{v}\\ \dot{\omega}\end{bmatrix}=\begin{bmatrix}v\cos\psi\\ v\sin\psi\\ \omega\\ (u_v-v)/\tau_v\\ (u_\omega-\omega)/\tau_\omega\end{bmatrix}, \tag{15}$$

where (x, y) is the inertial position, ψ is the heading, v is the velocity, and ω is the yaw rate of the UA, τ_v and τ_ω are time constants taking account for the actuator delay, and u_v and u_ω are the commanded speed and turning rate, respectively, constrained by the following dynamic constraints of the UA:

$$|u_v - v_0| \le v_{\max}, \tag{16}$$

$$|u_\omega| \le \omega_{\max}, \tag{17}$$

where v_0 is a nominal speed of the UA.

3.2 Design of the guidance law

We assume that the target is instantaneously non-maneuvering at each sampling time, and $\alpha>1$, which means the speed of the UA is larger than that of the target. Define e as the angular error between the UA's current velocity vector $\boldsymbol{V}_1$ and the desired vector $\hat{\boldsymbol{V}}_1$. Then we have

$$e = \theta_1 - \hat{\theta}_1, \tag{18}$$

where e is the angular error between the UA's current velocity vector $\boldsymbol{V}_1$ and the desired vector $\hat{\boldsymbol{V}}_1$, and θ_1 and $\hat{\theta}_1$ are the current UA azimuth angle and desired azimuth angle, respectively (Fig. 2). To guide the UA, the guidance command u_ω for the turning rate is set using a curvature command as

$$u_\omega = \dot{\theta}_1, \tag{19}$$

where $\dot{\theta}_1$ is the turning rate. Considering the Lyapunov function candidate $V=e^2/2$, the derivative of V is

$$\dot{V} = e\dot{e}. \tag{20}$$

From Eq. (18), we can obtain

$$\dot{e} = \dot{\theta}_1 - \dot{\hat{\theta}}_1. \tag{21}$$

From Fig. 2, the relationship between the angles are given as

$$\dot{\theta}_{\mathrm{d1}} = -\dot{\theta}_{\mathrm{d}}, \tag{22}$$

$$\dot{\theta}_{\mathrm{dt}} = \dot{\theta}_{\mathrm{d}} - \dot{\hat{\theta}}_1, \tag{23}$$

since

$$\theta_{\mathrm{d1}} = \pi - \theta_{\mathrm{d}} - \theta_2, \tag{24}$$

$$\theta_{\mathrm{dt}} = \theta_{\mathrm{d}} - \hat{\theta}_1. \tag{25}$$

In the triangle constructed by $\{p_1, p_{\mathrm{t}}, p_{\mathrm{d}}\}$, applying the cosine law leads to

$$d_2^2 = d_r^2 + d_1^2 - 2d_r d_1 \cos\theta_{\mathrm{dt}}. \tag{26}$$

Combing Eqs. (6) and (26), we have

$$d_r(d_1\cos\theta_{\mathrm{dt}} + d_2\cos\theta_{\mathrm{d1}} - d_r) = 0. \tag{27}$$

According to Eq. (14), $d_r>0$, and we can determine

$$d_1\cos\theta_{\mathrm{dt}} + d_2\cos\theta_{\mathrm{d1}} = d_r. \tag{28}$$

Differentiating Eq. (28) leads to

$$\dot{\theta}_{\mathrm{dt}} = \frac{-\sin\theta_{\mathrm{d1}}}{\alpha\sin\theta_{\mathrm{dt}}}\dot{\theta}_{\mathrm{d1}} - \frac{1}{\alpha\sin\theta_{\mathrm{dt}}}\frac{\mathrm{d}}{\mathrm{d}t}\left(\frac{d_r}{d_2}\right). \tag{29}$$

According to Eq. (28), we have

$$\cos\theta_{\mathrm{dt}} = \frac{d_r}{d_1} - \frac{d_2}{d_1}\cos\theta_{\mathrm{d1}}. \tag{30}$$

Combining Eqs. (14) and (30), we have

$$\cos\theta_{\mathrm{dt}} = \frac{d_2\cos\theta_{\mathrm{d1}} + d_2\sqrt{\alpha^2-\sin^2\theta_{\mathrm{d1}}}}{d_1} - \frac{d_2}{d_1}\cos\theta_{\mathrm{d1}} = \frac{\sqrt{\alpha^2-\sin^2\theta_{\mathrm{d1}}}}{\alpha}. \tag{31}$$

Since

$$\sin^2\theta_{\mathrm{dt}}+\cos^2\theta_{\mathrm{dt}}=1, \tag{32}$$

combining Eqs. (31) and (32) leads to

$$\left|\sin\theta_{\mathrm{d1}}\right|=\alpha\left|\sin\theta_{\mathrm{dt}}\right|. \tag{33}$$

Differentiating Eq. (7), we can obtain

$$\frac{\mathrm{d}}{\mathrm{d}t}\left(\frac{d_r}{d_2}\right)=\frac{-\sin\theta_{\mathrm{d1}}\left(\dfrac{d_r}{d_2}\right)}{\dfrac{d_r}{d_2}-\cos\theta_{\mathrm{d1}}}\dot{\theta}_{\mathrm{d1}}=\frac{\sin\theta_{\mathrm{d1}}\left(\dfrac{d_r}{d_2}\right)}{\dfrac{d_r}{d_2}-\cos\theta_{\mathrm{d1}}}\dot{\theta}_{\mathrm{d}}. \tag{34}$$

So, Eq. (29) can be expressed as

$$\dot{\theta}_{\mathrm{dt}}=\frac{\sin\theta_{\mathrm{d1}}\cos\theta_{\mathrm{d1}}}{\alpha\sin\theta_{\mathrm{dt}}\sqrt{\alpha^2-\sin^2\theta_{\mathrm{d1}}}}\dot{\theta}_{\mathrm{d1}}=\lambda\theta_{\mathrm{d1}}\dot{\theta}_{\mathrm{d1}}, \tag{35}$$

where $\left|\lambda\theta_{\mathrm{d1}}\right|\le 1/\alpha$. Combining Eqs. (22), (23), and (35), we have

$$\dot{\hat{\theta}}_{\mathrm{l}}=(1+\lambda\theta_{\mathrm{d1}})\dot{\theta}_{\mathrm{d}}. \tag{36}$$

Differentiating Eq. (2) leads to

$$\dot{\hat{\boldsymbol{t}}}_1=\frac{1}{\alpha}\left[\frac{\mathrm{d}}{\mathrm{d}t}\left(\frac{d_r}{d_2}\right)\boldsymbol{t}_{\mathrm{d}}+\frac{d_r}{d_2}\dot{\boldsymbol{t}}_{\mathrm{d}}+\dot{\boldsymbol{t}}_2\right]=\dot{\hat{\theta}}_{\mathrm{l}}\hat{\boldsymbol{n}}_1, \tag{37}$$

where $\hat{\boldsymbol{n}}_1$ is the unit normal vector of $\hat{\boldsymbol{t}}_1$. Owing to the assumption that the target is non-maneuvering at the sampling time, $\dot{\boldsymbol{t}}_2=0$. So, Eq. (37) turns into

$$\dot{\hat{\boldsymbol{t}}}_1=\frac{1}{\alpha}\left[\frac{\mathrm{d}}{\mathrm{d}t}\left(\frac{d_r}{d_2}\right)\boldsymbol{t}_{\mathrm{d}}+\frac{d_r}{d_2}\dot{\boldsymbol{t}}_{\mathrm{d}}\right]=\dot{\hat{\theta}}_{\mathrm{l}}\hat{\boldsymbol{n}}_1. \tag{38}$$

Substituting Eq. (34) into Eq. (38), we have

$$\frac{1}{\alpha}\left(\frac{d_r/d_2\sin\theta_{\mathrm{d1}}}{d_r/d_2-\cos\theta_{\mathrm{d1}}}\boldsymbol{t}_{\mathrm{d}}+\frac{d_r}{d_2}\boldsymbol{n}_{\mathrm{d}}\right)\dot{\theta}_{\mathrm{d}}=(1+\lambda\theta_{\mathrm{d1}})\dot{\theta}_{\mathrm{d}}\hat{\boldsymbol{n}}_1, \tag{39}$$

where $\boldsymbol{n}_{\mathrm{d}}$ is the normal vector of $\boldsymbol{t}_{\mathrm{d}}$. Taking a norm of both sides of Eq. (39), we have

$$\left|1+\lambda\theta_{\mathrm{d1}}\right|=\frac{\dfrac{1}{\alpha}\dfrac{d_r}{d_2}\sqrt{(d_r/d_2)^2-2\cos\theta_{\mathrm{d1}}(d_r/d_2)+1}}{\left|d_r/d_2-\cos\theta_{\mathrm{d1}}\right|}. \tag{40}$$

According to Eq. (7), we have

$$\left(\frac{d_r}{d_2}\right)^2-2\frac{d_r}{d_2}\cos\theta_{\mathrm{d1}}+1=\alpha^2. \tag{41}$$

Substituting Eq. (41) into Eq. (40) leads to

$$\left|1+\lambda\theta_{\mathrm{d1}}\right|=\frac{d_r/d_2}{\left|d_r/d_2-\cos\theta_{\mathrm{d1}}\right|}. \tag{42}$$

According to Eqs. (14) and (42), we obtain

$$-\left(1+\frac{1}{\alpha}\right)\le 1+\lambda\theta_{\mathrm{d1}}\le 1+\frac{1}{\alpha}. \tag{43}$$

Then by the guidance law to UA, the turning rate $\dot{\theta}_{\mathrm{l}}$ is set as

$$\dot{\theta}_{\mathrm{l}}=-\left(1+\frac{1}{\alpha}\right)|\dot{\theta}_{\mathrm{d}}|\,\mathrm{sign}(e)-k_{\mathrm{p}}e-k_{\mathrm{d}}\dot{e}, \tag{44}$$

where $\dot{\theta}_{\mathrm{d}}$ is the tangent line rate to the standoff circle, the proportional gain $k_{\mathrm{p}}>0$, and the derivative gain $k_{\mathrm{d}}>0$.

As shown in Fig. 2, the calculation of $\dot{\theta}_{\mathrm{d}}$ can be started from the following relation:

$$\theta_{\mathrm{d}}=\theta_{\mathrm{s}}-\theta_{\mathrm{t2}}. \tag{45}$$

From Fig. 2, the following equation holds:

$$\tan\theta_{\mathrm{t2}}=R_0/d_r. \tag{46}$$

Differentiating Eq. (46) gives

$$\dot{\theta}_{\mathrm{t2}}=-(R_0/r^2)\dot{d}_r. \tag{47}$$

Differentiating Eq. (45) and combining Eq. (47), we obtain

$$\dot{\theta}_{\mathrm{d}}=\dot{\theta}_{\mathrm{s}}+(R_0/r^2)\dot{d}_r. \tag{48}$$

Since Eqs. (18) and (36) hold, we have

$$\dot{e}=\dot{\theta}_{\mathrm{l}}-\dot{\hat{\theta}}_{\mathrm{l}}=\dot{\theta}_{\mathrm{l}}-(1+\lambda\theta_{\mathrm{dl}})\dot{\theta}_{\mathrm{d}}. \tag{49}$$

Using Eqs. (44) and (49), we have

$$\dot{e}=\frac{1}{1+k_{\mathrm{d}}}\left[-\left(1+\frac{1}{\alpha}\right)|\dot{\theta}_{\mathrm{d}}|\operatorname{sign}(e)-k_{\mathrm{p}}e-(1+\lambda\theta_{\mathrm{dl}})\dot{\theta}_{\mathrm{d}}\right]. \tag{50}$$

Substituting Eq. (50) into Eq. (20) leads to

$$\begin{aligned}\dot{V}=e\dot{e}=\frac{e}{1+k_{\mathrm{d}}}\Big[&-(1/\alpha+1)|\dot{\theta}_{\mathrm{d}}|\operatorname{sign}(e)\\&-(1+\lambda\theta_{\mathrm{dl}})\dot{\theta}_{\mathrm{d}}\Big]-\frac{k_{\mathrm{p}}e^2}{1+k_{\mathrm{d}}}\le 0.\end{aligned} \tag{51}$$

Note that $\dot{V}$ is negative semi-definite. The UA will be directed to encircle the standoff circle.

The differential geometry based guidance law is efficient when the UA is outside the standoff circle. When the UA is inside the standoff circle, however, this algorithm is not applicable due to the lack of tangent lines. Although several approaches can be suggested for this case, such as adopting a hybrid strategy to take advantage of both TVFG and LVFG (Chen *et al.*, 2013) and using modified control command (Prevost *et al.*, 2009), in this study we propose a simple and effective strategy. That is, when the courses of the UA and the target are different, the UA keeps current heading angles until the UA reaches the standoff circle; otherwise, the UA turns $\Delta\psi$ degrees diverging from the target (Fig. 3), which can shorten the time needed to reach the standoff distance.

3.3 Control of relative spacing

It is important to control the relative phase angle among the multiple UAs. We do not know where the target will go when it is in motion. Moreover, UAs need to control the phase angle in order to avoid a collision between the UAs. Therefore, the best solution is maximizing the sensor coverage to the target and keeping the phase angle between the various UAs (Fig. 4). Frew *et al.* (2008) proposed an additional phasing with a scaling term, and Lim *et al.* (2013) introduced a method based on the transformation of the vector field with variable R_0. Their similarity lies in speed control. Here we introduce how to control the relative phase angle.

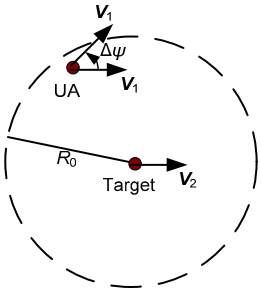

Fig. 3 Heading strategy when UA is inside the standoff circle

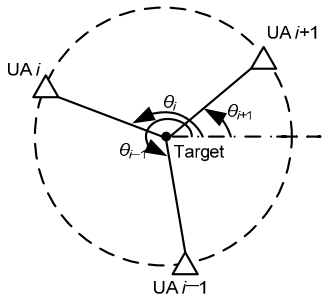

Fig. 4 Phase angle coordination between UAs

As shown in Fig. 4, phase angle coordination can be attained by controlling the UA speed proportional to the phase angle error. The phase angle offset is defined as

$$\Delta\theta=\theta_{i-1}-\theta_i, \tag{52}$$

where θ_{i-1} is the phase angle of the $(i-1)$th UA, and θ_i is the phase angle of the ith UA. Define ϕ_{d} as the desired phase angle offset. We adopt speed control to regulate the phase angle offset. Note that if all phase offsets between each two adjacent UAs are controlled to be $2\pi/n$ for n UAs, the target can be monitored from all directions. Consider the Lyapunov candidate

$$V_{\mathrm{p}}=(\Delta\theta-\phi_{\mathrm{d}})^2. \tag{53}$$

The derivative of V_{p} is

$$\frac{\mathrm{d}V_{\mathrm{p}}}{\mathrm{d}t}=2(\Delta\theta-\phi_{\mathrm{d}})(\dot{\theta}_{i-1}-\dot{\theta}_i). \tag{54}$$

For coordination of two UAs, we choose the angular speed commands as

$$\begin{cases}\dot{\theta}_1=-K_{\mathrm{p}}(\theta_1-\theta_2-\phi_{\mathrm{d}})-K_{\mathrm{d}}\Delta\dot{\theta}+\dfrac{v_1}{R_0},\\ \dot{\theta}_2=K_{\mathrm{p}}(\theta_1-\theta_2-\phi_{\mathrm{d}})+K_{\mathrm{d}}\Delta\dot{\theta}+\dfrac{v_2}{R_0},\end{cases}\tag{55}$$

where the proportional gain $K_{\mathrm{p}}>0$, the derivative gain $K_{\mathrm{d}}>0$, v_1 is the speed of the first UA, and v_2 is the speed of the second UA. When $v_1=v_2=v_0$, substituting Eq. (55) into Eq. (54) gives

$$\frac{\mathrm{d}V_{\mathrm{p}}}{\mathrm{d}t}=\frac{-4K_{\mathrm{p}}}{1+2K_{\mathrm{d}}}(\Delta\theta-\phi_{\mathrm{d}})^2\le 0.\tag{56}$$

Note that $\dot{V}_{\mathrm{p}}$ is negative semi-definite. This ensures that $\Delta\theta$ exponentially converges to the desired phase offset ϕ_{d}. Then the corresponding speed commands are

$$\begin{cases}u_{v_1}=-K_{\mathrm{p}}R_0(\theta_1-\theta_2-\phi_{\mathrm{d}})-K_{\mathrm{d}}R_0\Delta\dot{\theta}+v_1,\\ u_{v_2}=K_{\mathrm{p}}R_0(\theta_1-\theta_2-\phi_{\mathrm{d}})+K_{\mathrm{d}}R_0\Delta\dot{\theta}+v_2.\end{cases}\tag{57}$$

For coordination of three UAs, the corresponding speed commands are

$$\begin{cases}u_{v_1}=-K_{\mathrm{p}}R_0(\theta_1-\theta_2-\phi_{\mathrm{d}})-K_{\mathrm{d}}R_0\Delta\dot{\theta}+v_1,\\ u_{v_2}=v_2,\\ u_{v_3}=K_{\mathrm{p}}R_0(\theta_2-\theta_3-\phi_{\mathrm{d}})+K_{\mathrm{d}}R_0\Delta\dot{\theta}+v_3.\end{cases}\tag{58}$$

4 Simulation results

This section provides the simulation results using the proposed guidance law for coordinated standoff tracking of multiple UAs against a moving target. The target is assumed to move at a constant speed of 10 m/s. In the case of a two-UA team, phase offset $\phi_{\mathrm{d}}=\pi$, standoff distance $R_0=300$ m, and $\omega_{\max}=0.3$ rad/s. The resultant trajectories for the different numbers of UAs are shown in Fig. 5. Fig. 5a shows the case of two UAs following a moving target, keeping a desired standoff distance as well as a desired phase offset. Fig. 5b shows the case of three UAs cooperatively tracking a moving target.

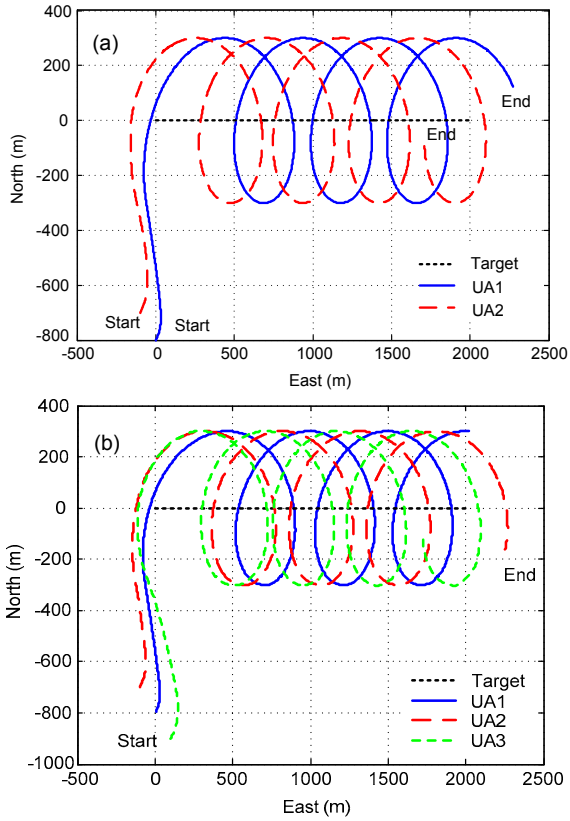

Fig. 5 Standoff tracking of different numbers of UAs to the target

(a) Coordinated tracking trajectories of two UAs ($\phi_{\mathrm{d}}=\pi$, $R_0=300$ m, $\omega_{\max}=0.3$ rad/s); (b) Coordinated tracking trajectories of three UAs ($\phi_{\mathrm{d}}=2\pi/3$, $R_0=300$ m, $\omega_{\max}=0.3$ rad/s). The target moves at a constant speed of 10 m/s

In the case of a three-UA team, the desired phase offset is chosen as $\phi_{\mathrm{d}}=2\pi/3$. Fig. 6 shows the phase angle offsets among the three UAs. The simulation parameters needed for the proposed guidance algorithm can be found in Table 1.

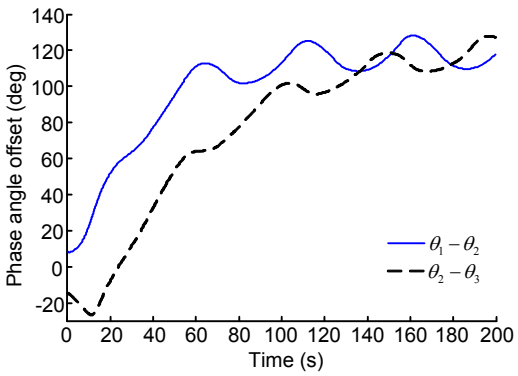

Fig. 6 Phase angle offset among the three UAs

Table 1 Simulation parameters

Parameter	Value
ϕ_d	π rad
v_0	40 m/s
R_0	300 m
v_{max}	10 m/s
ω_{max}	0.3 rad/s
τ_v, τ_ω	1/3
k_p, k_d	(2, 20)
K_p, K_d	(0.1, 5/3)

Capabilities of the proposed algorithm and the algorithm proposed by Oh *et al.* (2013) are compared. Performance comparisons in terms of the standoff distance and phase angle difference are shown in Figs. 7a and 7b, respectively. The proposed algorithm shows a good tracking performance in terms of the standoff distance error and phase angle offset error. The feasible ranges of k_p, k_d, K_p, and K_d are 0.8 to 70, 3 to 64, 0.04 to 3.75, and 0 to 6.5, respectively. It is clear that better tracking performance can be achieved by adding a derivative term. In general, the derivative action is useful in shortening the period of the loop and consequently hastening its recovery from disturbances (Li *et al.*, 2006). It can decrease the overshoot and steady-state error, and improve the stability.

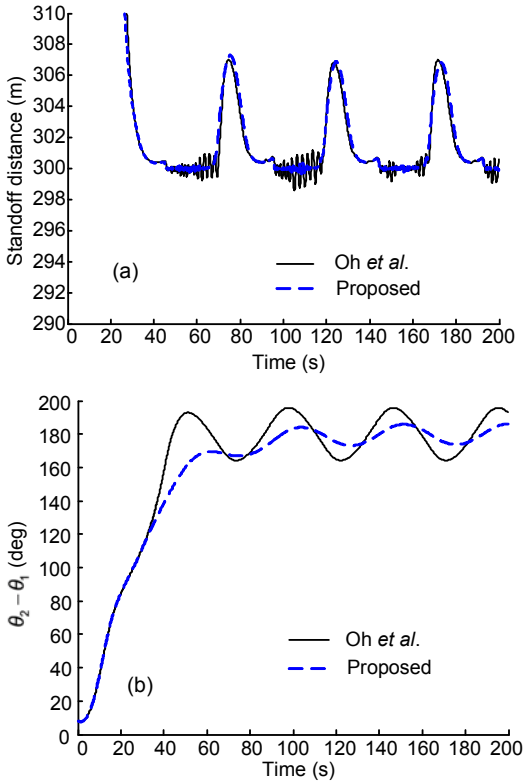

Fig 7 Comparison of standoff distance (a) and phase angle offset (b) between Oh *et al*. (2013)'s algorithm and our proposed algorithm

5 Conclusions

The topic of this paper is the coordinated standoff tracking strategy for multiple UAs. Differential geometry is applied to solve this problem. Using the relative geometry between the target and the UA, a convergent solution was obtained when the speed ratio of the UA to the target is larger than one. The convergent solution was then used to guide the UA into standoff tracking geometry. We extended the investigation to improve the tracking performance and proposed an improved guidance law ensuring a stable standoff tracking against a moving target based on differential geometry. The proposed guidance law showed a good tracking performance having the advantage of easy stability analysis by using a geometric relationship and the Lyapunov theory. The proposed approach was mathematically analyzed. It is easy to implement in embedded devices. Our contribution consists of improving the performance of keeping the desired standoff distance and phase angle difference. Oh *et al*. (2013) proposed an algorithm to maintain the desired standoff distance, to which we added a derivative term. Simulation results demonstrated the efficiency and robustness of the proposed algorithm. As a future work, the differential geometry based approach will include the adaptive control term considering target maneuvering.

References

Acevedo, J.J., Arrue, B.C., Maza, I., *et al.*, 2013. Cooperative large area surveillance with a team of aerial mobile robots for long endurance missions. *J. Intell. Robot. Syst.*, **70**(1-4):329-345. [doi:10.1007/s10846-012-9716-3]

Chen, H., Chang, K., Agate, C.S., 2013. UAV path planning with tangent-plus-Lyapunov vector field guidance and obstacle avoidance. *IEEE Trans. Aerosp. Electron. Syst.*, **49**(2):840-856. [doi:10.1109/TAES.2013.6494384]

Forsmo, E.J., Grotli, E.I., Fossen, T.I., *et al.*, 2013. Optimal search mission with unmanned aerial vehicles using mixed integer linear programming. Int. Conf. on Unmanned Aircraft Systems, p.253-259. [doi:10.1109/ICUAS.2013.6564697]

Frew, E.W., Lawrence, D.A., Morris, S., 2008. Coordinated standoff tracking of moving targets using Lyapunov guidance vector fields. *J. Guid. Contr. Dynam.*, **31**(2): 290-306.

Griffiths, S.R., 2006. Remote Terrain Navigation for Unmanned Air Vehicles. MS Thesis, Brigham Young University, Utah, USA.

Kim, S., Oh, H., Tsourdos, A., 2013. Nonlinear model predictive coordinated standoff tracking of a moving ground vehicle. *J. Guid. Contr. Dynam.*, **36**(2):557-566. [doi:10.2514/1.56254]

Lawrence, D.A., 2003. Lyapunov vector fields for UAV flock coordination. 2nd AIAA Unmanned Unlimited Conf., Workshop, and Exhibit, p.1-8. [doi:10.2514/6.2003-6575]

Lawrence, D.A., Frew, E.W., Pisano, W.J., 2008. Lyapunov vector fields for autonomous unmanned aircraft flight control. *J. Guid. Contr. Dynam.*, **31**(5):1220-1229. [doi:10.2514/1.34896]

Li, Y., Ang, K.H., Chong, G.C.Y., 2006. PID control system analysis and design. *IEEE Contr. Syst.*, **26**(1):32-41. [doi:10.1109/MCS.2006.1580152]

Lim, S., Kim, Y., Lee, D., *et al.*, 2013. Standoff target tracking using a vector field for multiple unmanned aircrafts. *J. Intell. Robot. Syst.*, **69**(1-4):347-360. [doi:10.1007/s10846-012-9765-7]

Nelson, D.R., Barber, D.B., McLain, T.W., *et al.*, 2007. Vector field path following for miniature air vehicles. *IEEE Trans. Robot.*, **23**(3):519-529. [doi:10.1109/TRO.2007.898976]

Nigam, N., Bieniawski, S., Kroo, I., *et al.*, 2012. Control of multiple UAVs for persistent surveillance: algorithm and flight test results. *IEEE Trans. Contr. Syst. Technol.*, **20**(5):1236-1251. [doi:10.1109/TCST.2011.2167331]

Oh, H., Kim, S., Shin, H.S., *et al.*, 2013. Rendezvous and standoff target tracking guidance using differential geometry. *J. Intell. Robot. Syst.*, **69**(1-4):389-405. [doi:10.1007/s10846-012-9751-0]

Ping, J.T.K., Ling, A.E., Quan, T.J., *et al.*, 2012. Generic unmanned aerial vehicle (UAV) for civilian application. IEEE Conf. on Sustainable Utilization and Development in Engineering and Technology, p.289-294. [doi:10.1109/STUDENT.2012.6408421]

Prevost, C.G., Theriault, O., Desbiens, A., *et al.*, 2009. Receding horizon model-based predictive control for dynamic target tracking: a comparative study. AIAA Guidance, Navigation, and Control Conf., p.1-9. [doi:10.2514/6.2009-6268]

Summers, T.H., Akella, M.R., Mears, M.J., 2009. Coordinated standoff tracking of moving targets: control laws and information architectures. *J. Guid. Contr. Dynam.*, **32**(1): 56-69. [doi:10.2514/1.37212]

White, B.A., Zbikowski, R., Tsourdos, A., 2007. Direct intercept guidance using differential geometry concepts. *IEEE Trans. Aerosp. Electron. Syst.*, **43**(3):899-919. [doi:10.1109/TAES.2007.4383582]

Wise, R.A., Rysdyk, R.T., 2006. UAV coordination for autonomous target tracking. Proc. AIAA Guidance, Navigation, and Control Conf., p.3210-3231. [doi:10.2514/6. 2006-6453]

Zarea, M., Pognonec, G., Schmidt, C., *et al.*, 2013. First steps in developing an automated aerial surveillance approach. *J. Risk Res.*, **13**(3-4):407-420. [doi:10.1080/13669877.2012.729520]